O^{5+} Observations From Various Solar Wind Speeds

Heiner Grünwaldt [1], Martin Hilchenbach [1], Matthias R. Aellig [2], Fred M. Ipavich [3], Kay-Uwe Reiche [4], Dieter Hovestadt [5], and Berend Wilken [1]

[1] *Max-Planck-Institut für Aeronomie, D-38191 Katlenburg-Lindau, Germany*
[2] *Physik. Inst, Universität Bern, Sidlerstr.5, CH-3012 Bern, Switzerland*
[3] *Dept.of Phys. and Astron., Univ.of Maryland, College Park, MD 20742, USA*
[4] *IDA, Techn. Univers. Braunschweig, D-38106 Braunschweig, Germany*
[5] *Max-Planck-Institut für Extraterr. Physik, D-85740 Garching, Germany*

Abstract. A first measure of O^{5+} abundance was recently published (5) on the basis of Ulysses data in a high speed solar wind stream. The favourable conditions of first months of SOHO exposed to an essentially undisturbed slow interstream solar wind in combination with the high sensitivity of the CELIAS/CTOF instrument made it possible to extend this result through a variety of speeds from 295 km/s up to 565 km/s. The ratios of O^{6+} (O^{7+}) with respect to O^{5+} turn out between 520 and 280 (275 and 12) , and seem to extrapolate smoothly down to the published Ulysses values.

INTRODUCTION

The recent observations of the O^{5+} UV emission lines by SOHO instrumentation (1,2) has revived demands for a widened knowledge of oxygen charge states throughout coronal expansion. While O^{6+} and O^{7+} as the dominant states in the solar wind have been measured through a large variety of solar wind conditions (3), the observation was usually restricted to these components by reason of statistics and resolution. The extension towards O^{5+} would not only enlarge the radial baseline for coronal and solar wind modelling from the evidence that can be given by plasma in situ observations; it would also close that link to the UV optical observations from various coronal heights that are restricted to O^{5+} as the only suitable oxygen emission line (4). The first and so far unique measure of O^{5+} in the solar wind was obtained 1998 by Wimmer et al. (5) using long time integration Ulysses data under sufficiently stable conditions of a high speed stream. The density ratio of O^{6+}/O^{5+} was found around 185, and referred to an electron temperature of $T_{O6,5+}=1.075\cdot10^6$K at the freezing-in distance, in close agreement with the simultaneous value of $T_{O7,6+}$.

During the first months of SOHO nominal operation the instrument CTOF (6) had collected solar wind heavy ion data predominantly originating from interstream regions of the solar minimum corona. This collection looked promising to determine an oxygen charge distribution extending down to include O^{5+} for a wide range of solar wind interstream conditions in terms of speed parameters of about 295-565 km/s. To use CTOF data for this purpose takes advantage not only of the large aperture of this instrument, but of the favourable conditions at the SOHO observatory position close to the sun, and constantly facing the solar wind ion stream. In spite of this advantage, values of the very low abundance of O^{5+} anticipated in the order of only 0.1-1% of total oxygen (7) still need extended data integration: the solar conditions around a pronounced activity minimum essentially free of transient events during the first months of SOHO operation in 1996 provided a suitable basis for this study.

CTOF as part of the particle instrument package CELIAS (6) derives spectral information of flux, energy, mass and charge of the solar wind heavy ion component by means of the time-of-flight technique combined with an electrostatic analyzer and post-acceleration, in the energy/charge (E/q) range from very low to 35.7 keV/q.

DATA PROCESSING AND ANALYSIS

Within nominal cycles, the E/q spectrum is scanned down starting from top at steps spaced by 4.094% and measured for each 2.35s. Before reaching E/q regions saturated by solar wind peak alphas and protons, the scans will turn to *Halt* and rest for the remaining cycle. The E/q, τ, and E readings of any one registered ion (PHA events) are the most accurate record since they bear the maximum resolution possible by the instrument. In the contour plot of Fig.1 a subframe of PHA results are displayed in a field of M/q and E around the expected position of O^{5+}. The M/q axis is denoted as *REF*, since the assignment of E/q and τ readings to M/q slightly varies with the overlapping signatures of the contributing species. For the same reason, the mass identification on the y-axis is still represented by the original

E channel numbers. The contour levels are selected to start from the 1 count level up in increments of $2^{½}$.

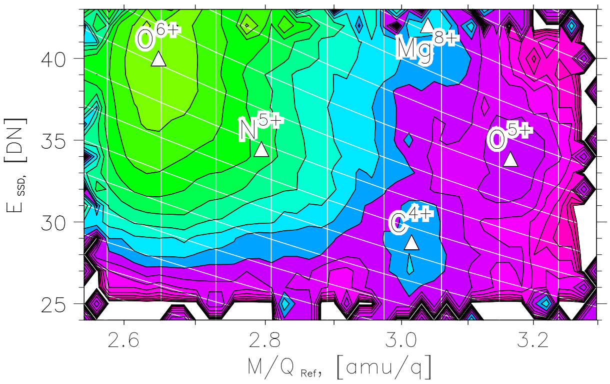

FIGURE 1. Accumulated PHA for V_{SW}=485 km/s, at U_{acc}=23 kV, in a field of M/Q_{Ref} and measured energy in digital units. M/Q_{Ref} assumes a generalized foil loss of 2.1 keV/e for all ions. All events are taken around E/Q close to the peak position of O^{5+}. The contour levels are spaced by a factor of $2^{½}$.

Since the frozen-in charge distribution as an indicator of the conditions in the source region can be expected to vary with solar wind status itself, we tried to establish the relative O^{5+} abundance as a function of the speed, V_{sw}. A selection of 27 classes with each 10 km/s bandwidth for the actual range of available speeds, 295-565 km/s, still promised statistical significance down to a density threshold of about $<10^{-7}$ cm^{-3}. For the classification, one hour averages of the solar wind bulk speed were available from the Proton Monitor (PM), a subsystem of the CELIAS package (9). For Fig.1 V_{sw}=485 km/s data are used.

Although only E/q channels close to the O^{5+} maximum are considered here, and O^{5+} turns out well resolved at this speed, there is evidently a large contribution from the thermal width of some neighbours like C^{4+} and the unresolved bulk of Mg^{8+} and Si^{9+}, and from the still dominant superthermal tail of O^{6+}. The positions marked for these ions are based on best knowledge of the $\tau=\tau(M,E_0)$ and $E=E(M,\tau)$ relation from flight and spare model laboratory measurement and from flight data evaluation.

While in the O^{5+} study of (5) similar PHA records from Ulysses data could be utilized, the ion rate within CTOF is much higher, with the consequence that PHA event counting becomes saturated well before reaching the proton/alpha *Halt* by the limits set by available data transmission capacity at all moderate to high flux ranges of the E/q spectrum. Especially the significance of rare ion counts competing with dominant neighbours is severely reduced. To cope with this enhanced data influx, a two-dimensional network of counters works in addition to the flight data system, called the Matrix Elements, ME (6). This network of a total of 1608 elements is seen as white lines in Fig.1. On board, a certain differential range of M/q and M is associated with every cell by a DPU process; here the boundaries are drawn as they appear in the original energy signal. It is capable to store all ion events up to electronic dead time limits with resolutions (3.3% resp. 7.2%) at least 3-4 times better than the FWHM of the actual profiles of τ and E. Since this resolution is the best available next to the original PHA, the system of ME is taken as the base for O^{5+} extraction.

Deconvolution of the ME system

In preceding publications the charge distribution of all major Fe ions (10) and the O^{7+}/O^{6+} ratio (11) have been derived as dominant constituents on top of a background of minority contributions. In comparison, the present task contrasts as surrounding ion populations contribute with substantial quantities to the matrix elements that contain O^{5+}. Therefore, it is not only for the immediate neighbours as C^{4+}, O^{6+}, Mg^{8+}, $Si^{8+,9+}$, but for the account of overlapping distributions of second order ions. As part of the task to deconvolve the system of all solar wind ion contributions, a total of 23 ion species in the range of M=12..28 was considered.

Particular care had to be taken for an improved account of the profiles in terms of τ and E, both in the peak position and in the profile shape. Refined calibration using the CTOF identical Spare Model were performed with beams of He, C, N, O, Ne_{20}, Ne_{22}, Ar, and Kr ions at the Lindau accelerator, with specific emphasis on the τ profiles; flight model calibration and in-flight data were used for confirmation and cross check, and for the E profiles under realistic noise environment. The profiles of both τ and E could be established far into the wings on both ends, and it was found that more refined models than the previous ones used by (11) had to be applied.

In the example of Fig.2, a measured τ profile is shown, and compared with the modelled approximations. For E, a Gaussian wing (low) and a kappa distribution (high), and for τ a Gaussian wing (low) and a Lorentzian (high) proved superior to any other approach. The χ^2 test between measurement and models confirmed this choice with satisfactory numbers of reduced χ^2 of the order of 1. Since for both energy and TOF profiles there are only weak accounts for the ion mass compared with the ones for central E and τ interpolation of the intermediate species seemed justified. Compared to previously published efficiency figures (e.g. 11) additional corrections were made to

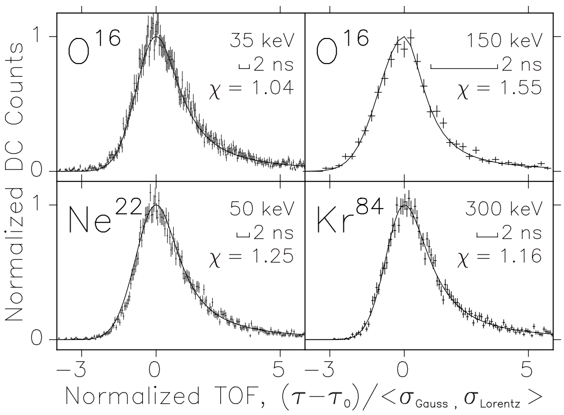

FIGURE 2. TOF profiles from CTOF/SM calibration at Lindau, normalized by the averaged low/high σ for Gaussian resp. Laurentzian wings. Based on a globally fitted approach for $\sigma_{G(auss)}{}^{*}$ and $\sigma_{L(orentz)}{}^{**}$ that depends primarily on the central τ and less on the ion mass, this asymmetric model is shown to match with good χ^2 checks over a wide range of mass and energy. Counts are given with statistical scatter. The actual τ scale is seen by the bars. Typical O^{6+},O^{5+} separation at solar wind is about 6σ.

$$* \; lg\, \sigma_G = -10^{-4} \; [0.35\,(\tau_0 - 391.1)\,(\tau_0 - 63.5) + 3.1 M]$$

$$** \; lg\, \sigma_L = 2.37\, lg \frac{\tau_0}{67.1} \; lg \frac{\tau_0}{9.67} + 0.0023\, M]$$

account for a fringe field effect between entrance system and TOF unit that favours the transmission of lower E/q values.

Using a transformation function that represents all these elements, the solar wind ion distribution function was mapped into the resulting PHA events per cycle versus E/q, τ, and E, and then applying the original flight classification algorithm these PHA were assigned to a simulated ME system, $\boldsymbol{M_{mod}}$. The simulation used convected Maxwellians for the ions, with averaged speeds taken from the Proton Monitor, and also the temperatures, modified by factors between $M^{1/2}$ and M. A weight factor allowed for the E/q step coverage with respect to the *Halt* level record.

Under the conditions described, $\boldsymbol{M_{mod}}$ only depends on the total of N densities, ρ_v, of the ions, ν. With $\boldsymbol{M^0_{mod}}$ normalized to unit densities, ρ_v can then be determined by optimizing the system:κ=1,K denote the indices of a subset of K=329 matrix elements relevant for the

$$M_{meas,\kappa} - \sum_{\nu=1}^{N} 10^{lg\,\rho_\nu}\; M^0_{mod,\nu,\kappa} = \delta_\kappa \;;\; \kappa = 1,K \qquad \textbf{(1)}$$

evaluation. In order to account for the overlap of ion profiles that may cause spurious interference from species beyond the immediate neighbourhood of O^{5+}, the selected boundary encloses all ions from mass 12 to 28 with their predominant charge status. He and Fe beyond either end are well separated; the fully stripped CNO are included for completion, but with only marginal influence. Of the remaining N=23 species: $C^{4..6+}$, $N^{5..7+}$, $O^{5..8+}$, $Ne_{20}{}^{6..8+}$, $Ne_{22}{}^{8+}$, $Mg^{7..10+}$, $Si^{8..12+}$, some (as $Ne^{6..7+}$) turn out negligible, some (as Mg^{8+}, Si^{9+}) add up to a common profile rather than being resolved.

Searching for the minimum of $\Sigma\delta_\kappa^2$ as the optimum of system eq.1 the ρ_v have to obeye the system of eq.2:where μ=1,23. This is solved in two steps: in the

$$\sum_{\nu=1}^{N}\sum_{\kappa=1}^{K} 10^{lg\,\rho_\nu}\, M^0_{mod,\mu,\kappa}\, M^0_{mod,\nu,\kappa} = \sum_{\kappa=1}^{K} M_{meas,\kappa}\, M^0_{mod,\mu,\kappa} \qquad \textbf{(2)}$$

first step, the linear equivalent is inverted, with the condition of ρ_v enforced non-negative, yielding a zero approach of densities. In the second step, starting at this zero approach (zero ρ_v starting with $10^{-7.5}$) the non-linear system (eq.2) is solved using Broyden‘s formalism (12). While with this two-step approach it is already likely to avoid being trapped at relative minima of the problem, this is tested for by variation of the starting vector.

For error analysis, three roots of uncertainties have been considered: (1) statistics of the matrix element accumulation, (2) remaining uncertainty of the E and τ calibration, (3) remaining uncertainty of the profile parameters. Since looking at relative abundance, uncertainties of the efficiency can be neglected. Within these margins, the deconvolution process has been repeated in order to get the O^{5+} error bars.

OBSERVATION AND DISCUSSION

In Fig.3 the ratios of O^{6+} and O^{7+} with respect to O^{5+} are shown in terms of proton speed. At the top of the frame the freezing-in temperature, $T_{O7,6+}$, taken as an average profile from these constituents is denoted as a rough classification of the corona involved. $T_{O7,6+}$ has been derived using the compilation of ionisation and recombination rate data of Arnaud and Rothenflug (13). Of these two major constituents O^{6+} is seen as dominant throughout most of the speed range. The highest temperature, at 295 km/s, is seen evidently still below the value of about $2.1 \cdot 10^6$K where the two charges are in balance. With rising speed O^{7+} decreases by more than a factor 10, with a

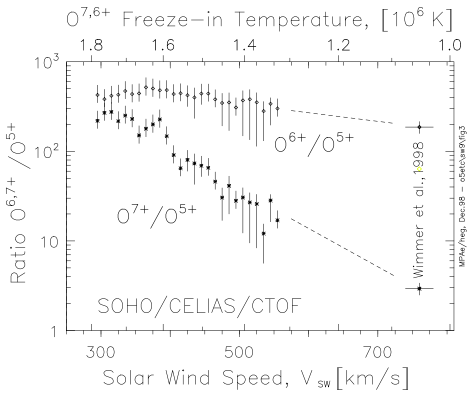

FIGURE 3. Ratios of O^{6+}/O^{5+} and O^{7+}/O^{5+} (CELIAS) versus solar wind speed, 295-565 km/s at 10 km/s bins, complemented by a fast stream Ulysses result. Error bars include statistical errors and systematic uncertainties. The freeze-in temperature taken from O^{6+}/O^{7+} on top indicates the status of the coronal base.

corresponding decrease of the freeze-in temperature down to about $1.35 \cdot 10^6$K. This trend confirms the results derived from a subset of CTOF data by (11) and is discussed in terms of speed being anti-correlated with $T_O^{7,6}$, the electron temperature at the corona base, and the local electron temperature gradient in (10). When this trend shows a gradual change of conditions from pronounced slow interstream wind towards marginal high speed stream, the trend is evidently confirmed by the long time average around a high 760±20 km/s that has been added to the figure from 150 days of Ulysses data as the only observation of O^{5+} so far (6). The dashed line that is fitted using both these data of low and high speed streams is tentatively drawn in order to demonstrate the connection, and it is also used to extrapolate the temperature scale written on top.

The major cause for the error bars are both statistical and systematic errors involved in the O^{5+} abundance deconvolution as summarized above. The appreciable amount of uncertainty up to an order of factor 2 reflects the still difficult task. The increase of errors towards faster speeds reflects the larger overlap by ion neighbours at the higher kinetic ion temperatures.

In general the ratios of O^{6+}/O^{5+} and O^{7+}/O^{5+} follow the expected trend with solar wind speed and freeze-in temperature. Some obvious deviations from this trend underline that the dependency is not unique, since other parameters beside the freezing-in temperature will eventually result in a certain proton speed. On the basis of these long time averages individual situations on a time scale of days can be looked into, with a specific emphasis to understand the derived temperatures involving O^{5+} in comparison with SOHO/UVCS results in streamers. When based on a combined evaluation of the ME data used, and the CTOF matrix rates that bear E/q spectral information at however more restricted M and M/q, an improved accuracy on a shorter timescale can be expected.

ACKNOWLEDGEMENTS

CELIAS is supported in part by DLR, Germany, by the PRODEX program of ESA, and by NASA.

REFERENCES

1. Wilhelm, K., Lemaire, P., and SUMER team, *Solar Physics,* **170,** 75-104 (1997)
2. Raymond, J. C., Kohl, J. L., and UVCS team, *Solar Physics,* **175**, 645-665 (1997)
3. von Steiger, R., "Composition of the Solar Wind", in *Cosmic Winds and the Heliosphere*, edited by Jokipii, Sonett, and Giampapa, U. Arizona Press, 1997, 581-616
4. Kohl, J.L., *Solar Physics*, **175**, 613-644 (1997)
5. Wimmer-Schweingruber, R., von Steiger, R., Geiss J., Gloeckler G., Ipavich F. M., and Wilken B., "O^{5+} in High Speed Solar Wind Streams: SWICS/ULYSSES Results", in *Solar Composition and its Evolution - From Core to Corona*, edited by Fröhlich, Huber, Solanki, and von Steiger, Kluwer Academic Press, 1998, 387-396
6. Hovestadt, D., Hilchenbach, M., Bürgi, A., Grünwaldt, H., Ipavich, F. M., Galvin, A. B., Bochsler, P., Reiche, K.-U., and CELIAS Team, *Solar Physics,* **162**, 441-481 (1995)
7. Aellig, M. R., *Freeze-in Temperatures and Relative Abundances of Iron Ions in the Solar Wind Measured With SOHO/CELIAS/CTOF,* PHD Thesis, U. Bern, 1998
9. Ipavich, F. M., Galvin A. B., Lasley S. E., Paquette, J. A., Hefti, S., Reiche K., Coplan, M. A., Gloeckler, G., Bochsler, P., Hovestadt, D., and CELIAS Team, *J. Geophys. Res.,* **103**, 17205-17214 (1998)
10. Aellig, M. R., Grünwaldt, H., Bochsler, P., Hovestadt, D., Reiche, K.-U., and CELIAS Team, *J. Geophys. Res.,* **103**, 17215-17222 (1998)
11. Hefti, S., *Solar Wind Freeze-in Temperatures and Fluxes Measured with SOHO/CELIAS/CTOF and Calibration of the CELIAS Sensors*, PHD Thesis, U. Bern, 1997
12. Press, W.H., Teukolsky, S.A., Vetterling, W.T., and Flannery, B.P., *Numerical Recipies*, Cambridge U. Press, 1992, 382-386
13. Arnaud, M. and Rothenflug, R., *Astron. & Astrophys. Suppl. Ser.,* **60**, 425-457 (1985)